Measurement and calculation of absolute single- and multiple-charge-exchange cross sections for Fe^{q+} ions impacting CO and CO$_2$

J. Simcic,[1] D. R. Schultz,[2] R. J. Mawhorter,[3] I. Čadež,[4] J. B. Greenwood,[5] A. Chutjian,[1] C. M. Lisse,[6] and S. J. Smith[7]

[1]*Atomic and Molecular Physics Group, Jet Propulsion Laboratory, California Institute of Technology, Pasadena, California 91109-8099, USA*

[2]*Physics Division, Oak Ridge National Laboratory, Oak Ridge, Tennessee 37831-6372, USA*

[3]*Department of Physics and Astronomy, Pomona College, Claremont, California 91711, USA*

[4]*Joef Stefan Institute, 1000 Ljubljana, Slovenia*

[5]*Physics Department, Queen's University, Belfast BT7 1NN, United Kingdom*

[6]*Space Department, Applied Physics Laboratory, Johns Hopkins University, Laurel, Maryland 20732, USA*

[7]*Physics Department, Indiana Wesleyan University, Marion, Indiana 46953, USA*

Absolute cross sections are reported for single, double, and triple charge exchange of Fe^{q+} ($q = 5$–13) ions with CO and CO$_2$. The highly charged Fe ions are generated in an electron cyclotron resonance ion source. Absolute data are derived from knowledge of the target gas pressure, target path length, and incident and charge-exchanged ion currents. Experimental results are compared with new calculations of these cross sections in the n-electron classical trajectory Monte Carlo approximation in which the ensuing radiative and nonradiative cascades are approximated with scaled hydrogenic transition probabilities and scaled Auger rates. The present data are needed in astrophysical applications of solar- and stellar-wind charge exchange with comets, planetary atmospheres, and circumstellar clouds.

PACS number(s): 34.50.Gb, 82.30.Fi, 96.60.Vg

I. INTRODUCTION

Charge exchange (CE) of highly charged ions with neutral targets is not only important from fundamental, theoretical aspects [1] but is also an important charge-reduction process affecting the ionization fraction of fusion [2] and astronomical [3] plasmas. The detection of x rays from solar system targets is in part because of CE of highly charged solar wind or magnetospheric ions with cometary gases [4], the Martian exosphere [5], Jupiter's upper atmosphere [6], and interstellar He [7,8].

Given the inherent uncertainties of observations, such as solar-wind and magnetospheric-projectile abundance, target-gas abundance, charge-exchange cross sections, and atmospheric attenuation, one would like to have, for modeling purposes, as many laboratory-measured quantities as possible. To this end, single and multiple absolute CE cross sections have been previously reported for relevant projectile-target pairs and results compared with those of available theoretical and semiempirical calculations [9–12]. Presented in this article are absolute CE cross sections for the species Fe$^{(5-13)+}$ interacting with the cometary and atmospheric species CO and CO$_2$. While Fe ions have a relatively small abundance (less than 3% of the total oxygen-ion abundance), these heavier species, along with ions of C, N, O, Ne, Mg, Si, and S, give rise to the observed comet and planetary x-ray emissions associated with CE. The experimental approach is summarized in Sec. II, and theoretical considerations are discussed in Sec. III. Results and comparisons with the n-electron, classical trajectory Monte Carlo (nCTMC) method and the extended over-barrier model are given in Sec. IV, and conclusions are given in Sec. V.

II. EXPERIMENTAL CONSIDERATIONS

The present data were acquired using the electron cyclotron resonance (ECR) ion source and the CE x-ray-detection beam line at the JPL Highly Charged Ion (HCI) Facility. Details of the beam lines, the CE geometry, system calibration, and experimental errors have been given previously [9,10]. In terms of the CE gas cell, all measurements were taken with the largest cell exit aperture diameter consistent with maintaining adequate gas density in the cell; limiting pressure gradients at the ion exit-aperture region so as to reduce CE outside the geometric path length of the cell; and maintaining a high angular collection efficiency of the charge-exchanged ions. The choice of gas-cell exit aperture was determined in separate measurements of ^{3}He^{2+} charge exchanging with He and H$_2$ where the scattering kinematics introduced a large angular spread in the CE products [13]. Those data ensured that collection-angle effects were negligible in the present data. All measurements were carried out at an Fe^{q+} energy of $7q$ keV. The ion currents depend on the Fe charge state and were in the range 4 pA–50 nA.

Separate tests were carried out to search for effects of metastable levels of the projectile ions on the final results, and these are described in Refs. [9–12]. As a check, the ions Fe^{7+} and Fe^{8+} were generated by several paths. In one path, each was formed and extracted in the usual fashion from the ECR source. In the second, Ar quenching gas was introduced into a long section of the beam line between the 90° charge/mass selection magnet and the electrostatic "Y" deflector [10,11]. As a third, Fe^{7+} was generated, starting from ECR-extracted Fe^{8+} ions, by the process Fe^{8+} + Ar $\rightarrow$ Fe^{7+} + Ar$^+$, and Fe^{8+} was similarly generated by the step Fe^{9+} + Ar $\rightarrow$ Fe^{8+} + Ar$^+$ [9]. Absolute CE cross sections measured in the collisions with CO were the same, within experimental error, for the Fe^{7+} and Fe^{8+} ions produced in the three paths. Since one would expect a different distribution of metastable states in the different formation processes, the results indicate that the same starting state—almost certainly the ground state—was present in measurements with the Fe^{q+} ions.

Measurement errors were calculated by adding in quadrature the statistical errors, taking into account the number of measurements for each ion-molecule pair, errors in measuring the gas density, the ion current ratios, absolute currents, the effective gas-cell collision length (corrected for gas streaming), and current fluctuations of the ion beams. The final convoluted 2σ errors in the data are given in Table I. The errors averaged to 13% ($\sigma_{q,q-1}$), 21% ($\sigma_{q,q-2}$), and 25% ($\sigma_{q,q-3}$).

III. THEORETICAL CONSIDERATIONS

The processes contributing to the measured CE cross sections in collisions of an Fe^{q+} ion with target molecule A-B can be summarized as

$$Fe^{q+} + A\text{-}B \rightarrow Fe^{(q-j)+} + A\text{-}B^{(j+s)+} + se, \quad (1)$$
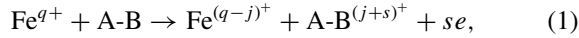
where $j + s$ is the number of electrons transferred from the target, j is the number of electrons captured by the projectile, and s is the number of free electrons produced by the collision. In the present case, captures up to $j = 3$ have been measured, with no determination made as to whether the A-B$^{(j+s)+}$ species remains as a parent ion or subsequently decays to excited, fragment ions. One-electron capture occurs mainly to a high n-state of $Fe^{(q-1)+}$, which stabilizes through a series of photon emissions. In the case of two- or three-electron transfers, one, two, or three electrons may be in excited states. The resulting excited ion stabilizes either by photon emission or autoionization. For example, single transfer ($j + s = 1$, $s = 0$) and autoionizing double transfer ($j + s = 2$, $s = 1$) will contribute to $\sigma_{q,q-1}$. Double transfer ($j = 2$, $s = 0$), single-autoionizing triple transfer ($j = 3, s = 1$), and double-autoionizing quadruple transfer ($j = 4$, $s = 2$) will contribute to $\sigma_{q,q-2}$.

A full quantum-mechanical treatment of low to intermediate energy collisions between HCIs and molecules remains a daunting theoretical challenge. Fortunately, charge transfer in such collisions proceeds mostly to relatively highly excited states, and hence simpler and more tractable approaches may be used to calculate the $\sigma_{q,q-j}$ cross sections. The method employed here is the nCTMC approach [14,15]. This approximation was previously used to describe single electron capture (SEC) in Ne^{10+} + He, Ne, Ar, CO, and CO_2 collisions [16]. It was also used to describe multiple electron capture in N^{7+} and O^{7+} + CO, CO_2, and H_2O collisions in which good agreement was found with results from cold-target, recoil-ion momentum spectroscopy measurements [17].

The CTMC method describes an ion-atom or ion-molecule collision through consideration of a large number of trajectories chosen from an ensemble of projectile-target configurations that simulate the initial quantum-mechanical electronic probability distributions for position and momentum [18,19]. The subsequent particle motions are determined by solving the classical equations of motion. At an asymptotic final separation, one calculates the relative electron energies to each of the ionic centers to determine what, if any, transition has occurred (i.e., elastic scattering, excitation, charge transfer, and ionization). In particular, for charge transfer, the classical orbital states of the captured electrons can be mapped to the corresponding quantum states using appropriate binning rules [20–22]. Results are generally progressively better for

capture to higher principal quantum numbers, as expected from the correspondence principle. This is the regime in which fully quantum-mechanical methods have significant difficulty and is to a reasonable extent the regime of capture channels considered here.

CTMC was originally formulated with a treatment of only a single, active electron on the target. Various forms of the independent-electron model (IEM) were used to describe multiple electron processes such as transfer ionization or multiple electron capture. However, a key insight [14] that led to the development of nCTMC was that multiple-electron processes in collisions of HCIs with atoms are more appropriately modeled if the target electrons possess the correct sequential binding energies, as opposed to equivalent binding energies used in IEM approaches. Thus, in the nCTMC method for ion-atom collisions, the experimentally observed ionization potentials are used for the n-electron binding energies. In this article, the target molecules are considered as single centers with eight active electrons. The approximation of a single center is reasonable at the collision velocities considered, especially given the high charge state of the Fe^{q+} projectiles. The binding energy of the first of the eight electrons is given by the experimentally observed first ionization potential and that of the next seven electrons by cumulative orbital energies [23]. Finally, the electrons interact with the target center through a model potential approximated as that of the dominant element (oxygen) in CO and CO_2. Future work could refine this approach by placing the electrons into initial orbits of a multicentered molecular target.

For each of the nine Fe^{q+} ions colliding with CO and CO_2, approximately 20 000 projectile ion trajectories of collision energy of $7q$ keV were computed and binned. The resulting events led to one-, two-, three-, or fourfold capture. The ion cores were treated as being frozen, and the interaction between the cores and active target electrons were given by the model potential of Refs. [24,25]. Because of the structure of the Fe^{q+} projectiles, it was necessary to determine the quantum states after capture by the non-Coulomb binning method [22] instead of the usual method applicable to fully stripped ions [20]. For the higher charge states, capture proceeds dominantly to about $n = 6$, and for the lower charge states to $n = 4$, roughly in accord with the usual scaling $n_{max} \sim q^{3/4}$. The distribution of capture is significant up to about $n = 10$. While SEC is the largest channel, double (DEC), triple (TEC), and quadruple electron capture (QEC) are also significant. Therefore, since capture is often to multiply excited states, it is necessary to simulate the ensuing radiative and nonradiative (autoionizing) cascades. This results in a final charge- and quantum-state distribution that would be observed in an experiment where the scattered Fe^{q+} ions are detected at a distance from the target molecules, having traveled a time sufficient for radiative and nonradiative cascades to transpire.

A full treatment of these cascades presents a significant challenge requiring quantum-structure and radiative and nonradiative (Auger and Coster-Kronig transition) data for all levels up to $n = 10$ for Fe^{2-11+} (i.e., up to fourfold capture in Fe^{5-13+}). While data exist for part of these sets of levels and transitions, they are almost exclusively for low-lying states. Therefore more schematic models of ion quantum levels were created, and scaled hydrogenic transition probabilities

TABLE I. Absolute single and multiple CE cross sections for $Fe^{(5-13)+}$ ions colliding with CO and CO_2. Ionization potentials are given in the first column for each target. Projectile energies are $7q$ keV. The second entry in each cell is the calculated cross section in the present nCTMC approximation. See Figs. 1–6 for comparisons with error limits on both experimental and theoretical results. All cross sections are in units of 10^{-15} cm^2 and errors are cited at the 2σ level.

Target (I_P)	Process	Projectile								
		Fe^{5+}	Fe^{6+}	Fe^{7+}	Fe^{8+}	Fe^{9+}	Fe^{10+}	Fe^{11+}	Fe^{12+}	Fe^{13+}
CO (14.01 eV)	$\sigma_{q,q-1}$	4.00 ± 0.60 3.21	4.20 ± 0.62 3.75	5.07 ± 0.38 4.36	5.03 ± 0.37 5.17	5.50 ± 0.82 5.75	6.40 ± 0.98 6.24	8.35 ± 1.04 6.77	7.84 ± 0.84 7.15	9.35 ± 1.06 7.43
	$\sigma_{q,q-2}$	– 0.404	– 0.531	1.68 ± 0.25 0.628	1.56 ± 0.21 0.422	1.70 ± 0.37 0.589	1.90 ± 0.40 0.695	1.59 ± 0.28 0.822	1.39 ± 0.26 0.899	1.91 ± 0.36 1.12
	$\sigma_{q,q-3}$	– 0.148	– 0.172	0.57 ± 0.14 0.188	0.58 ± 0.11 0.166	– 0.202	– 0.211	0.50 ± 0.18 0.208	0.68 ± 0.15 0.280	0.40 ± 0.09 0.328
CO_2 (13.77 eV)	$\sigma_{q,q-1}$	3.20 ± 0.50 3.34	3.80 ± 0.58 3.83	3.60 ± 0.61 4.51	3.80 ± 0.62 5.32	5.30 ± 0.80 5.90	7.06 ± 0.77 6.47	7.56 ± 0.83 7.02	8.02 ± 0.89 7.25	9.32 ± 1.08 7.72
	$\nu\sigma_{q,q-2}$	1.30 ± 0.34 0.397	1.40 ± 0.28 0.554	1.30 ± 0.33 0.656	1.20 ± 0.30 0.534	1.60 ± 0.43 0.582	1.79 ± 0.34 0.762	1.79 ± 0.34 0.817	1.68 ± 0.34 0.899	1.68 ± 0.35 1.13
	$\sigma_{q,q-3}$	– 0.157	– 0.188	0.40 ± 0.09 0.218	0.60 ± 0.24 0.198	0.70 ± 0.19 0.214	0.79 ± 0.16 0.240	0.99 ± 0.24 0.255	0.99 ± 0.25 0.325	0.97 ± 0.24 0.414

and scaled Auger rates [26] were used. The cascades were computed for double, triple, and quadruple capture events in a multiply excited state following the general, well-known procedure [27] for treatment of multiple Auger electron emission and fluorescence in plasmas. A more detailed and accurate model would clearly require a more extensive effort that would be justified only if more accurate input data from a treatment better than nCTMC were available. As described subsequently, estimates are given as to the uncertainty of final calculated results arising from approximations in the cascade models.

IV. RESULTS AND DISCUSSION

Absolute single ($\sigma_{q,q-1}$), double ($\sigma_{q,q-2}$), and triple ($\sigma_{q,q-3}$) CE cross sections for the Fe^{q+} ions colliding with CO and CO_2 are listed in Table I. Results of the nCTMC calculation and the radiative/Auger cascade processing for the nine iron ions colliding with CO are shown in Fig. 1 (SEC), Fig. 2 (DEC), and Fig. 3 (TEC). Good agreement of the theoretical results with the measurements is seen. In particular, the magnitude and trend of the results for SEC agree well with the measurements but tend to underestimate magnitudes for the lower and higher qs. The nCTMC results for SEC also display a smoother trend, whereas the measurements vary somewhat from the trend for several charge states, possibly reflecting details not included in the collision or cascade models. The theoretical results for DEC also agree well with measurements in that they are both nearly constant for all charge states, but the theoretical data are about a factor of 2–3 smaller in magnitude. Similarly, the nCTMC plus cascade results for TEC are nearly flat. This is in agreement with experiment, but here the very small values of the measured data vary above and below the theoretical values.

The error limits associated with the theoretical results are estimates of the minimum and maximum contributions
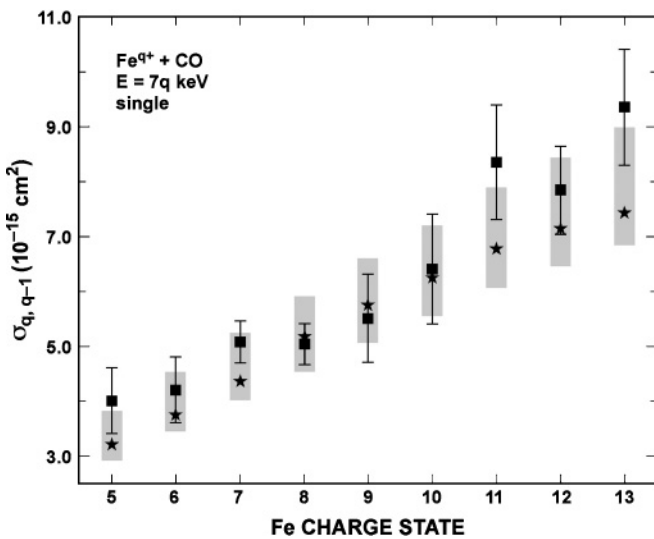

FIG. 1. Results of the nCTMC calculation and radiative/Auger cascade processing for CE in Fe^{5-13+} collisions with CO (star) compared with the present experiments (square). Shown are the single CE results with error bars representing the maximum estimated uncertainty from the cascade model. See also listings in Table I.
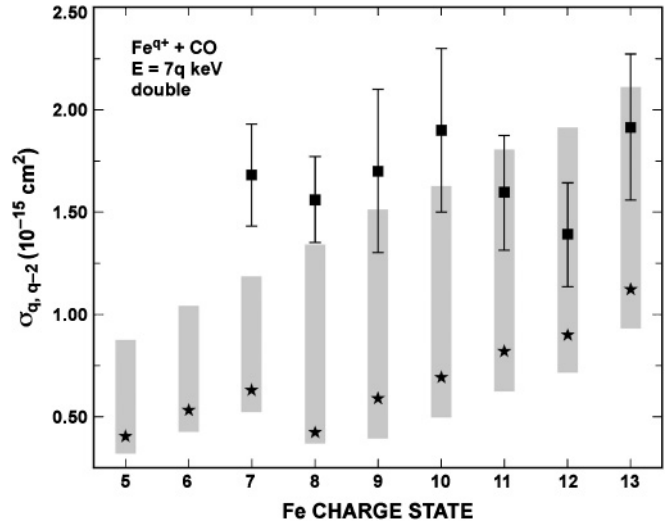

FIG. 2. Same as for Fig. 1, but for the double CE results.

possible from the cascade process. Specifically, for SEC, the maximum is given by the calculated direct SEC cross section plus 100% of the DEC and estimated maximum fractions of the TEC and QEC undergoing cascade added to the SEC result. The minimum is given by assuming complete stabilization of the multiple electron capture computed by nCTMC in the DEC, TEC, and QEC channels. These represent the extremes of the contributions from cascades that could raise or lower the SEC results. Similarly, for DEC the maximum is found by adding to the direct nCTMC DEC cross section the estimated largest contributions from TEC and QEC and the minimum by assuming complete stabilization of the TEC and QEC inputs to the cascade. The same approach is used to estimate cascade errors for TEC. It should be noted that these error bars do not reflect approximations inherent to the nCTMC model but rather only uncertainties in the cascade following the initial multiply excited population from that calculation.

For the dominant process, SEC, these estimates of the maximum uncertainty due to the radiative and nonradiative cascade processing could change the direct single capture
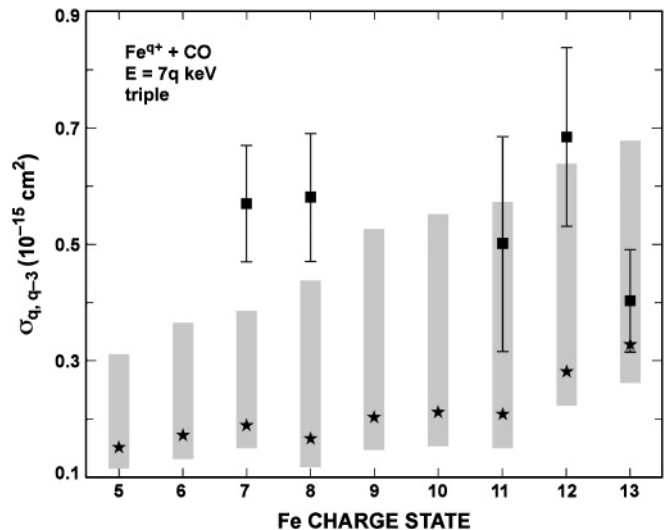

FIG. 3. Same as for Fig. 1, but for the triple CE results.

cross sections computed with the present nCTMC model by at most about $+20\%$ and -10%. This indicates that the uncertainty stemming from the estimation of the very large array of radiative and nonradiative rates for each of the Fe ions for levels up to as high as $n = 10$ contributes no more than these amounts. It shows the adequacy of the present approach given the underlying limitation of the CTMC method to produce the input distribution for the cascade. Whereas the uncertainty in the radiative and nonradiative cascade relevant to final SEC states depends predominantly on two-electron rates, those required to estimate the contribution from these processes for DEC and TEC require predominantly three- and four-electron rates of considerably greater uncertainty. The presently estimated uncertainties for the DEC and TEC channels are commensurately larger, being as much as $+100\%$ and -25%. We note that the model rates adopted as well as the underlying CTMC method cannot pick up subtle quantum structure effects that might cause an initial population or subsequent cascade to result in cross sections that vary significantly from the rather smooth trend that the theoretical results display. Clearly additional physical insight could be derived from measurements and calculations that treat the multiple capture and rearrangement process in more detail.

Shown in Fig. 4 are the experimental and theoretical results for single CE of Fe^{q+} ions with CO_2. Results for double and triple CE are shown in Figs. 5 and 6, respectively. There is again good overall agreement of the theoretical results with the magnitude and trends of the measurements. As for CO, the SEC measurements show more variations from the smooth trend predicted by the theoretical results, and the DEC results are again about a factor of 2–3 smaller than the measurements. Comparison of the theoretical results for the two targets indicates that the SEC and DEC results vary by only about 5% between CO and CO_2. This occurs because the
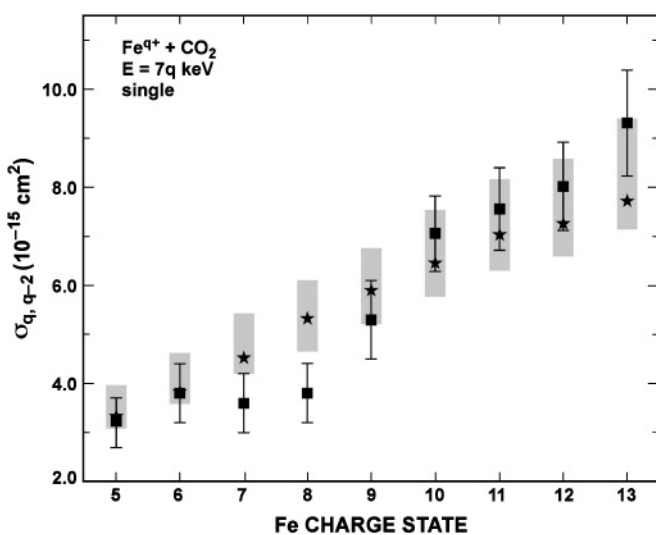

FIG. 5. Same as for Fig. 4, but for the double CE results.

sequential binding energies of CO and CO_2 are quite similar (e.g., for CO, 14.01, 29.03, 46.75, . . . eV, and for CO_2, 13.78, 28.65, 43.52, . . . eV); that is, for the HCIs considered here, the most critical parameter influencing the capture process is the electronic binding energy. One also notes that the rising trend of the SEC cross sections capture cross section increases with increasing q; i.e., the projectile presents a larger capturing sphere or impact parameter b for the higher charge states. For SEC, this occurs over a wide range of b, with the probability for capture peaking at small b. For DEC and TEC that occur over a smaller range of b, increases in q do not increase the multiple capture probability as much as they can for SEC, which has a smaller probability for capture that extends to larger b, yielding the much flatter dependence as a function of q.

Finally, while significantly less rigorous than the nCTMC theory, the semiempirical extended overbarrier model (EOBM) [28] and assumptions therein were used in a simple calculation of the relative fraction of the true capture channel versus the autoionizing multiple-capture channel for CO. The CO binding energies were taken from Refs. [29,30]. This is the same approach as in Ref. [10], where EOBM cross sections

FIG. 4. Results of the nCTMC calculation and radiative/Auger cascade processing for CE in Fe^{5-13+} collisions with CO_2 (star) compared with the present experiments (square). Shown are the single CE results with error bars representing the maximum estimated uncertainty from the cascade model. See also listings in Table I.
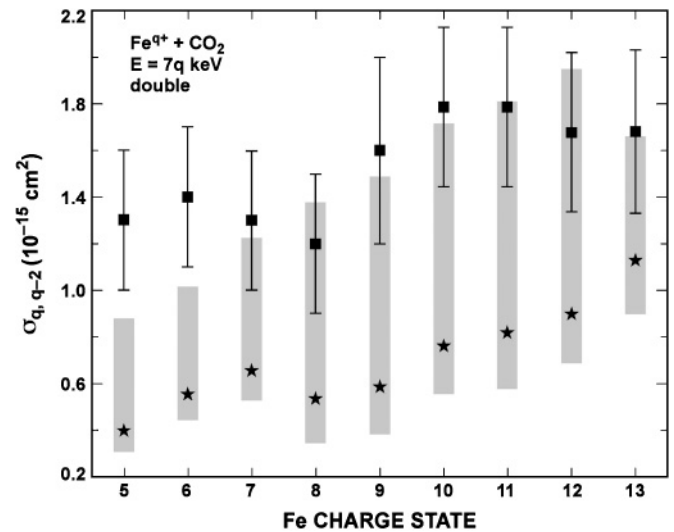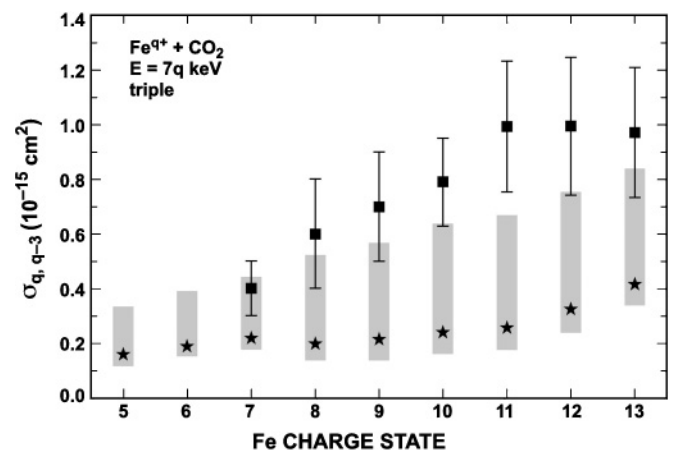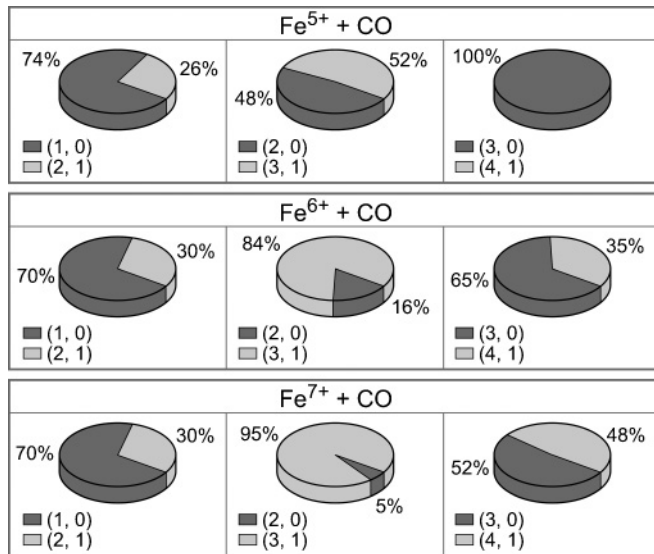

FIG. 6. Same as for Fig. 4, but for the triple CE results.

FIG. 7. Pie chart representing the fractions of true capture and autoionizing multiple captures for $Fe^{(5-7)+}$ ions with CO, as calculated in the extended overbarrier model. The legend $(j + s, s)$ refers to $j + s$ electron transfers followed by s electron autoionizations.

were calculated for the CO target for projectile C^{5+} and C^{6+} ions. Results of the EOBM approximation for CO and $Fe^{(5-7)+}$

for all excitation strings are shown in Fig. 7, where one sees a trend of increasing contribution from autoionizing multiple capture with increasing Fe^{q+} charge state.

V. CONCLUSIONS

Comparisons have been presented between experimentally measured absolute CE cross sections and the *n*-electron classical trajectory Monte Carlo (*n*CTMC) approximation for collisions of $Fe^{(5-13)+}$ ions with CO and CO_2. Results for capture of up to three electrons are given. There is agreement within combined experimental and theoretical error limits for $\sigma_{q,q-1}$ and agreement within error limits in most cases for the smaller cross sections $\sigma_{q,q-2}$ and $\sigma_{q,q-3}$. Such data are useful not only in assessing the state of theory but also in calculating ionization fractions in cometary and planetary atmospheres.

ACKNOWLEDGMENTS

[1] Y. Wu, Y. Y. Qi, S. Y. Zou, J. G. Wang, Y. Li, R. J. Buenker, and P. C. Stancil, Phys. Rev. A **79**, 062711 (2009).

[2] O. Marchuk, Y. Ralchenko, R. K. Janev, G. Bertschinger, and W. Biel, J. Phys. B **42**, 165701 (2009); A. W. Kleyn, N. J. Lopes Cardozo, and U. Samm, Phys. Chem. Chem. Phys. **8**, 1761 (2006).

[3] D. Koutroumpa, R. Lallement, V. Kharchenko, and A. Dalgarno, Space Sci. Rev. **143**, 217 (2009).

[4] S. Otranto, R. E. Olson, and P. Beiersdorfer, Can. J. Phys. **86**, 171 (2008); A. Bhardwaj *et al.*, Planet. Space Sci. **55**, 1135 (2007).

[5] K. Dennerl *et al.*, Astron. Astrophys. **451**, 709 (2006).

[6] Y. Hui, D. R. Schultz, V. A. Kharchenko, P. C. Stancil, T. E. Cravens, C. M. Lisse, and A. Dalgarno, Astrophys. J. **702**, L158 (2009).

[7] T. G. Slanger, T. E. Cravens, J. Crovisier, S. Miller, and D. F. Strobel, Space Sci. Rev. **139**, 267 (2008).

[8] D. Bodewits, R. Hoekstra, B. Seredyuk, R. W. McCullough, G. H. Jones, and A. G. G. M. Tielens, Astrophys. J. **642**, 593 (2006).

[9] I. Čadež, J. B. Greenwood, J. A. Lozano, R. J. Mawhorter, S. J. Smith, M. Niimura, and A. Chutjian, J. Phys. B **36**, 3303 (2003).

[10] R. J. Mawhorter, A. Chutjian, T. E. Cravens, N. Djurić, S. Hossain, C. M. Lisse, J. A. MacAskill, S. J. Smith, J. Simcic, and I. D. Williams, Phys. Rev. A **75**, 032704 (2007).

[11] N. Djurić, S. J. Smith, J. Simcic, and A. Chutjian, Astrophys. J. **679**, 1661 (2008).

[12] A. Chutjian, J. B. Greenwood, and S. J. Smith, *Applications of Accelerators in Research and Industry*, edited by J. L. Duggan and I. L. Morgan (Am. Inst. Phys., New York, 1999), p. 881.

[13] R. J. Mawhorter *et al.* (unpublished).

[14] R. E. Olson, J. Ullrich, and H. Schmidt-Böcking, Phys. Rev. A **39**, 5572 (1989).

[15] D. R. Schultz, R. E. Olson, C. O. Reinhold, S. Kelbch, C. Kelbch, H. Schmidt-Böcking, and J. Ullrich, J. Phys. B **23**, 3839 (1990).

[16] A. A. Hasan, F. Eissa, R. Ali, D. R. Schultz, and P. C. Stancil, Astrophys. J. **560**, L201 (2001).

[17] R. Ali, P. A. Neill, P. Beiersdorfer, C. L. Harris, M. J. Raković, J. G. Wang, D. R. Schultz, and P. C. Stancil, Astrophys. J. **629**, L125 (2005).

[18] R. Abrines and I. C. Percival, Proc. Phys. Soc. London **88**, 861 (1966).

[19] R. E. Olson and A. Salop, Phys. Rev. A **16**, 531 (1977).

[20] R. L. Becker and A. D. MacKellar, J. Phys. B **17**, 3923 (1983).

[21] M. J. Raković, D. R. Schultz, P. C. Stancil, and R. K. Janev, J. Phys. A **34**, 4753 (2001).

[22] D. R. Schultz, P. C. Stancil, and M. J. Raković, J. Phys. B **34**, 2739 (2001).

[23] [http://cccbdb.nist.gov/].

[24] R. H. Garvey, C. H. Jackman, and A. E. S. Green, Phys. Rev. A **12**, 1144 (1975).

[25] D. R. Schultz and C. O. Reinhold, Comput. Phys. Commun. **114**, 342 (1998).

[26] J. Burgdörfer, C. O. Reinhold, and F. Meyer, Nucl. Instrum. Methods Phys. Res. B **205**, 690 (2003).

[27] J. S. Kaastra and R. Mewe, Astron. Astrophys. Suppl. Ser. **97**, 443 (1993).

[28] A. Niehaus, Nucl. Instrum. Methods Phys. Res. B **23**, 17 (1987).

[29] G. Sampoll, R. L. Watson, O. Heber, V. Horvat, K. Wohrer, and M. Chabot, Phys. Rev. A **45**, 2903 (1992).

[30] H. O. Folkerts, T. Schlathölter, R. Hoekstra, and R. Morgenstern, J. Phys. B **30**, 5849 (1993).